Published in final edited form as:
Neuron. 2009 November 12; 64(3): 381–390. doi:10.1016/j.neuron.2009.08.035.

AMPA receptor incorporation into synapses during LTP: the role of lateral movement and exocytosis

Hiroshi Makino[1,2] and **Roberto Malinow**[1,2]

[1] Department of Neurosciences and Division of Neurobiology, University of California San Diego, La Jolla, CA 92093

[2] Watson School of Biological Sciences, Cold Spring Harbor Laboratory, Cold Spring Harbor, NY 11724

Summary

The regulated trafficking of AMPA receptors (AMPARs) to synapses is thought to underlie the enhanced transmission in long-term potentiation (LTP), a cellular model of memory. However, there is controversy regarding the non-synaptic site, either on the surface or intracellularly, from which AMPARs move into synapses during LTP. Using recombinant surface-fluorescent receptors in organotypic rat hippocampal slices, we show that the majority of AMPARs incorporated into synapses during LTP is from lateral diffusion of spine surface receptors containing GluR1, an AMPAR subunit. Following synaptic potentiation, AMPARs in intracellular pools containing GluR1 are driven to the surface primarily on dendrites. These exocytosed receptors likely serve to replenish the local extrasynaptic pool available for subsequent bouts of plasticity. These results clarify the role of intracellular and surface AMPARs during synaptic plasticity.

Introduction

AMPA-type glutamate receptors (AMPARs) mediate fast synaptic transmission at a majority of excitatory synapses and their accumulation within synapses is considered important for enhanced transmission during LTP (Bredt and Nicoll, 2003; Collingridge et al., 2004; Malinow and Malenka, 2002; Sheng and Kim, 2002; Shepherd and Huganir, 2007). In dendritic regions, AMPARs can be found in various non-synaptic compartments: 1) intracellularly in the dendrite; 2) intracellularly in the spine; 3) on the dendritic surface (which is generally lacking excitatory synapses); or 4) on the spine surface but outside the synapse (Petralia and Wenthold, 1992). Two routes that can be exploited for synaptic delivery of AMPARs are lateral diffusion from the surface (Adesnik et al., 2005; Ashby et al., 2006; Borgdorff and Choquet, 2002; Ehlers et al., 2007; Heine et al., 2008; Passafaro et al., 2001; Yang et al., 2008; Yudowski et al., 2007) and exocytosis from intracellular compartments (Gerges et al., 2006; Park et al., 2004; Park et al., 2006; Passafaro et al., 2001; Wang et al., 2008; Yang et al., 2008). The contribution of these two distinct processes to LTP has not been established, possibly because of the difficulty in monitoring these processes simultaneously in a preparation that shows robust LTP. To determine which path receptors use to reach synapses during synaptic plasticity, we imaged hippocampal pyramidal neurons in organotypic slices 2–3 days after expressing a red cytoplasmic marker

To whom correspondence should be addressed: Roberto Malinow (rmalinow@ucsd.edu).

(DsRed or tdTomato) along with individual AMPAR subunits (GluR1 or GluR2) tagged on their amino-terminus with a pH sensitive form of eGFP (Super Ecliptic pHluorin, SEP) (Figure 1B). Such tagging allows one to distinguish between surface receptors, which display green fluorescence, and intracellular receptors, which show no fluorescence (Ashby et al., 2004; Kopec et al., 2006; Sharma et al., 2006). SEP-tagging of receptor allows one to monitor exocytosis of receptors during plasticity. Selective photobleaching of SEP-tagged surface receptors allows one to measure the contribution of surface receptors to plasticity. Our results suggest that during LTP, AMPARs from non-synaptic sites on the spine surface move into the synapse by lateral movement. Exocytosis of intracellular AMPARs occurs, but minutes after LTP and primarily onto the dendritic shaft. These results elucidate the roles of receptor lateral movement and exocytosis during synaptic plasticity.

Results

Subunit-specific AMPAR mobility on spines before and after LTP

Using fluorescence recovery after photobleaching (FRAP), we first determined what fraction of the GluR1-SEP and GluR2-SEP signal on spines corresponds to recombinant receptors at synapses, rather than in an extrasynaptic spine surface pool (Figure 1A). Previous studies have shown that in CA1 pyramidal neurons of organotypic hippocampal slices, in the absence of neural activity, recombinantly expressed GluR2 is incorporated into synapses. Without activity, recombinant GluR1 does not go into synapses, but can be driven into synapses with LTP (Hayashi et al., 2000; Kopec et al., 2006; Shi et al., 2001). Single-particle tracking experiments on dissociated cultured neurons indicate that synaptic receptors are relatively immobile, while non-synaptic receptors on the spine surface readily interchange with dendritic receptors (Borgdorff and Choquet, 2002; Ehlers et al., 2007; Triller and Choquet, 2005). Thus, we reasoned that recombinant GluR1 should largely be mobile on spines (i.e. non-synaptic) in the absence of activity, and become immobile following LTP (i.e. synaptic). In contrast, some fraction of GluR2 should be immobile (i.e. synaptic) on spines even without activity (see Figures S1A and B in the Supplemental Data for schematic rationale). Under basal conditions, photobleaching spine SEP fluorescence to background levels (Figure 1B, see the Experimental Procedures) was followed by a recovery ($t_{½}$ = 1.2 ± 0.3 min, n = 14 for GluR1-SEP; $t_{½}$ = 1.8 ± 0.6 min, n = 17 for GluR2-SEP, p = 0.51) that was complete by 30 minutes for GluR1-SEP (103 ± 6%, n = 14) but not for GluR2-SEP (81 ± 3%, n = 17, p < 0.01 compared to GluR1-SEP, Figures 1C and D). Following chemical LTP (cLTP, which has been shown to increase excitatory synaptic amplitudes and spine volume in an NMDA receptor-dependent manner, and to drive recombinant GluR1 into synapses (Kopec et al., 2006; Kopec et al., 2007)), we detected an increase in spine volume (60 ± 20%, n = 21, p < 0.01 for GluR1-SEP-expressing cells; 71 ± 20%, n = 13, p < 0.05 for GluR2-SEP-expressing cells) accompanied by an increase in spine recombinant receptors (56 ± 30%, n = 21, p < 0.05 for GluR1-SEP; 23 ± 13%, n = 13, p = 0.19 for GluR2-SEP, Figures 1E and F). Importantly, GluR1-SEP on spines recovered to only 70 ± 4% of the pre-photobleach levels (n = 21, p < 0.01 compared to GluR1-SEP recovery without LTP, Figure 1G), whereas GluR2-SEP recovery was not affected by cLTP (77 ± 5%, n = 14, p = 0.51 compared to GluR2-SEP recovery without LTP, Figure 1H). These results indicate that the immobile fraction of fluorescent recombinant receptors on a spine behaves as predicted for synaptic receptors.

Input-specific reduction of AMPAR mobility on spines following LTP

A prominent feature of LTP is its input-specificity (Andersen et al., 1977). To examine how input-specific LTP induction alters the mobility of AMPARs on a spine, we used two-photon glutamate uncaging in conditions that permit NMDA receptor activation (bath contained low Mg^{2+} and tetrodotoxin, see the Experimental Procedures) to induce LTP at

individual spines (single-spine LTP, Figure 2A). Consistent with previous studies (Harvey and Svoboda, 2007; Matsuzaki et al., 2004), this led to a rapid structural potentiation (Figures 2B, C, E, G and S2 in the Supplementary Data) in spines (80 ± 17% for GluR1-SEP-expressing cells, n = 14, $p < 0.01$ compared to 4 ± 8% in nearby spines, n = 11; 79 ± 21% for GluR2-SEP-expressing cells, n = 8, $p < 0.05$ compared to 4 ± 12% in nearby spines, n = 8) that was accompanied by a comparable increase in spine GluR1-SEP (97 ± 35%, n = 14, $p < 0.01$ compared to −10 ± 7% in nearby spines, n = 11) and little increase in GluR2-SEP (20 ± 9%, n = 8, $p = 0.44$ compared to 8 ± 13% in nearby spines, n = 8). As seen following cLTP, FRAP of the spine after single-spine LTP demonstrated a significant immobile pool (i.e. synaptic pool) of GluR1-SEP receptors, which was 21 ± 6% of the post-potentiation spine fluorescence (Figure 2F; or 44 ± 14% of the pre-potentiation value, Figure S3A in the Supplemental Data). Reduction of GluR1 mobility (i.e. synaptic incorporation of GluR1) was input-specific, since FRAP of GluR1-SEP in nearby non-potentiated spines was nearly complete (97 ± 7%, n = 11, $p < 0.05$, Figures 2B, D and F). There was no increase in an immobile fraction of GluR2-SEP following single-spine LTP (FRAP was 79 ± 6%, n = 8 for potentiated spines; 72 ± 9%, n = 8 for nearby non-potentiated spines, $p = 0.51$, Figure 2H; see Figure S3B in the Supplemental Data for FRAP relative to the pre-potentiation fluorescence value). This conforms with previous studies suggesting that LTP is largely mediated by synaptic incorporation of GluR1-containing AMPARs (Hayashi et al., 2000; Shi et al., 2001; Zamanillo et al., 1999).

Small contribution of AMPAR exocytosis to synaptic potentiation during LTP

We wished to determine if AMPARs that incorporate into the synapse during LTP originate from the surface or from intracellular stores. To examine this, we expressed GluR1-SEP/GluR2-SEP and DsRed and photobleached a segment of dendrite along with its associated spines before inducing synaptic potentiation (Figures 3A and B). We confirmed that the SEP signal in low pH intracellular compartments was protected from such photobleaching. Bath application of NH_4Cl (which alkalinizes intracellular compartments (Ashby et al., 2006; Fernandez-Alfonso and Ryan, 2008)) produced a similar increase in SEP signal in neurons not exposed to photobleaching (19 ± 7% in dendrites, 7 cells and 13 ± 10% in spines, n = 17) as that seen in neurons after photobleaching (27 ± 4% in dendrites, 4 cells and 9 ± 6% in spines, n = 15; $p = 0.79$ for dendrites, $p = 0.43$ for spines; Figures S4A-E in the Supplemental Data). We reasoned that if LTP drives intracellular SEP-tagged receptors into synapses, following photobleaching of surface SEP-tagged receptors, LTP should produce a large increase in spine SEP fluorescence. However, if receptors driven into synapses by LTP originate from the surface, following photobleaching of surface SEP-tagged receptors, LTP should produce little fluorescence increase in spines.

First, we monitored fluorescence recovery of GluR1-SEP and GluR2-SEP on spines after photobleaching surface receptors on a dendritic segment (~25 μm) without LTP (Figure 3A). For both GluR1 and GluR2, recovery on a spine was much reduced compared to the recovery after photobleaching only spines (31 ± 3% for GluR1-SEP [compare with 103 ± 6% after photobleaching spines], n = 24; 23 ± 1% for GluR2-SEP [compare with 81 ± 3% after photobleaching spines], n = 43, Figure 3E and F). This suggests that the recovery of the spine mobile fraction observed with single-spine photobleaching was largely due to lateral movement of receptors originating from the surface of the dendrite.

To determine the degree of the contribution of AMPAR exocytosis during LTP, we initially used cLTP to induce synaptic potentiation at multiple spines. cLTP was induced immediately after photobleaching a dendritic segment (Figure 3A). We observed robust punctate appearance of GluR1-SEP, but only on the dendrite and not on spines (10 dendrites). These fluorescent spots only appeared after induction of cLTP and everywhere along the photobleached regions on a dendrite (Figures 3C and D). They could persist for

minutes (Figure 3C), similar to the time-course of dendritic exocytosis of synaptotagmin-IV (Dean et al., 2009), suggesting restricted diffusion following surface exposure. The cLTP-induced appearance of GluR1-SEP fluorescent spots was blocked by co-expression of botulinum neurotoxin serotype A light chain (BoNT/A-LC, Figure 3G), supporting the view that events represented surface exocytosis of compartments that contain GluR1-SEP.

Notably, following dendrite/spine photobleaching, recovery of GluR1-SEP fluorescence on spines was not greater with cLTP than the recovery without cLTP (without cLTP, 34 ± 4%, n = 24; with cLTP, 31 ± 3%, n = 33, p = 0.56, Figure 3E), suggesting small contribution of exocytosis to synaptic potentiation. We did not detect exocytosis of GluR2-SEP before or during cLTP (Figures 3C and D). The level of recovery of GluR2-SEP fluorescence on spines was independent of cLTP (without cLTP, 26 ± 1%, n = 43; with cLTP, 24 ± 2%, n = 31, p = 0.26, Figure 3F). These results suggest that AMPARs that incorporate into synapses during LTP contain GluR1 and originate from the spine or dendrite surface. Exocytosis of GluR1 occurs predominantly onto the dendrite and contributes little to synaptic potentiation.

Compartmentalized GluR1 exocytosis replenishing a local extrasynaptic AMPAR pool

We wished to use single-spine LTP, which permits greater temporal and spatial control than cLTP, to monitor exocytosis and surface mobility of AMPARs during synaptic plasticity. We tested only GluR1 since the results above suggested it to be the major subunit whose dynamic behavior is strongly affected during LTP. We photobleached a dendritic segment (~40 μm) along with spines (Figure 4A). We waited ~2 min until tdTomato (the cytoplasmic marker protein) returned to pre-photobleach levels. At this time, the SEP signal only partially recovered (9 ± 3%; n = 17). We then induced LTP in an individual spine, and monitored the subsequent increase in spine volume (tdTomato) and surface GluR1-SEP accumulation on the spine (~2 sec/frame, Figure 4B). Spines that were located closely to the middle of the photobleached region were selected for LTP to assure that a significant portion of SEP fluorescence recovery in spines is due to exocytosis and not to lateral diffusion from non-photobleached regions. Following LTP, spines increased in volume in a manner comparable to that seen in experiments with no photobleaching (63 ± 11% at 30 min, n = 9, $p < 0.01$ compared to −4 ± 4%, n = 8 in nearby non-potentiated spines, Figure 4C). As seen during cLTP, we detected some exocytotic events of GluR1-SEP primarily on dendrites. However, in contrast to the global LTP protocol mediated by cLTP, the glutamate uncaging-evoked GluR1 exocytosis was highly localized around potentiated spines (Figures 4B, F and G, see movie in the Supplemental Data). This suggests that underlying signaling events that lead to GluR1 exocytosis during LTP is compartmentalized to a stretch of dendrite (with length constant, $\lambda = 2.70$ μm). Furthermore, these events typically occurred after structural potentiation was observed (Figure 4B, H and I, mean time between last uncaging pulse and onset of exocytosis was 1.57 ± 0.17 min). If the receptors incorporated into synapses during LTP are derived from intracellular stores, the recovery of GluR1-SEP signal at potentiated spines should be more than the recovery of non-potentiated spines (which were chosen to be within ~5 μm from the potentiated spines). Indeed, given that the increase in immobilized GluR1-SEP (i.e. synaptic GluR1-SEP) after LTP is 44% of the pre-LTP spine fluorescence (Figure S3A in the Supplemental Data), the potentiated spine should recover to at least ~40% more than the non-potentiated spine (40% is an underestimate because exocytosed receptors should move to extrasynaptic regions of a spine as well as to a synapse if intracellular compartments provides receptors to spines.). Recovery of GluR1-SEP in potentiated spines was only slightly higher than nearby non-potentiated spines (35 ± 5%, n = 9, and 22 ± 4%, n = 8 at 30 min, respectively, $p < 0.05$, Figure 4D); had receptors from intracellular stores contributed to LTP, one would have expected > 60% (i.e. 40% + 22%) recovery in LTP spines. Furthermore, when normalized to spine volume, the fluorescence signal of GluR1-SEP was not different between potentiated and nearby non-potentiated

spines (22 ± 3%, n = 9, and 23 ± 4%, n = 8 at 30 min, respectively, p = 0.96, Figure 4E). These results suggest that intracellular GluR1 does not contribute to receptors incorporated into the synapse during LTP. Rather, once exocytosed to the surface of the dendrite during LTP, GluR1 passively diffuses into nearby spines and replenishes a local extrasynaptic pool of receptors leading to an equal density of extrasynaptic GluR1 on potentiated and non-potentiated spines. We note that because of the slow imaging rate of our experiments, there could be fast exocytotic events that we do not detect. However, this does not change the conclusion that receptors undergoing exocytosis (with any time-course) during LTP do not appreciably become lodged in the synapse.

Detecting exocytosis of endogenous AMPARs on dendrites following LTP

Our imaging experiments indicate that following glutamate uncaging-evoked LTP, there is a rapid spine enlargement followed by exocytosis of recombinant receptors onto the dendritic surface. We tested this model for endogenous AMPA receptors using combined patch-clamp recordings and two-photon glutamate uncaging. AMPAR-mediated currents were measured at the soma in a voltage-clamp mode (held at −60 mV) by uncaging glutamate onto a spine and onto a dendrite (located next to the spine of interest) of tdTomato-expressing CA1 pyramidal neurons. To induce LTP, we paired 30 uncaging laser pulses (at 0.5 Hz) with postsynaptic depolarization at 0 mV (Figure 5A). We then continued to monitor responses from the same spine and dendrite over 10 min. We saw a rapid increase in the spine response following LTP (n = 10) and the increase was stable at least for 10 min. Similar to a previous study (Andrasfalvy and Magee, 2004), dendrite responses also increased following LTP (138 ± 10 % at 10 min, n = 17, $p < 0.05$ compared to control, 103 ± 8 %, n = 7, Figure 5B and C), but the increase was delayed compared to the increase in the spine response. The time course of the change in dendrite response was similar to the exocytosis of recombinant GluR1-SEP (compare Figure 4H and 5B), suggesting that endogenous AMPARs behave similarly to recombinant GluR1. This increase in the dendrite response was unlikely due to stimulation of additional spine AMPARs since a) the increase in the dendrite and spine response showed different time-courses following LTP induction; and b) uncaging glutamate at a comparable distance as the dendrite, but on the opposite side of the potentiated spine produced minimal responses (< 10% of baseline responses). Consistent with previous studies (Harvey and Svoboda, 2007; Matsuzaki et al., 2004), the changes of spine volume were tightly correlated with the changes in the spine response (n = 9, r = 0.87, $p < 0.01$, Figure 5D). The changes in the spine response were also correlated with the changes in the dendrite response at 10 min (n = 10, r = 0.69, $p < 0.05$), but not at 1 min after LTP induction (n = 10, p = 0.16, Figure 5E) reinforcing the finding that the dendritic response potentiation was delayed compared to the spine response potentiation. These results support our view that endogenous AMPARs move to synapses immediately after LTP through lateral diffusion, and dendritic AMPARs are gradually replenished by exocytosis.

Lateral diffusion of AMPARs to synapses from spine surface during LTP

We wished to test directly whether the receptors that incorporate into synapses originate from the non-synaptic spine surface. To assess this possibility, we photobleached GluR1-SEP on a spine, then rapidly induced LTP at the same spine by glutamate uncaging, and subsequently monitored its fluorescence recovery. We reasoned that if non-synaptic spine surface GluR1-SEP moves to synapses during LTP, GluR1-SEP photobleached before LTP should become immobile (and thus irreplaceable by fluorescent GluR1-SEP) on spines. Thus, we should see less GluR1-SEP signal on spines compared to the amount seen after LTP without spine photobleaching. In contrast, if either the dendritic surface or intracellular compartments are the primary providers of synaptically targeted GluR1, LTP should lead to

the same GluR1-SEP signal in spines irrespective of spine photobleaching before LTP (see Figures S5A–D in the Supplemental Data for possible scenarios).

To compare the amounts of GluR1-SEP increase in spines across LTP experiments, we normalized by the increase in spine size. In the absence of photobleaching, 30 minutes following LTP, the GluR1-SEP signal and spine volume increased to similar amounts (ΔSEP/Δvolume = 108 ± 9% at 30 min, n = 14, Figures 6A, B and E). However, in spines receiving photobleaching before LTP induction, ΔSEP/Δvolume was 80 ± 7% at 30 min (n = 11, $p < 0.05$ compared to no photobleaching, Figures 6C, D and E). This shows that a significant amount of GluR1-SEP immobilized by LTP (which we showed above indicates synaptic incorporation) originated from the spine surface. In fact, the amount of immobile, photobleached GluR1-SEP at a spine following potentiation is approximately ~25% of the total GluR1-SEP (i.e. 1–80/108) on a spine. This value can fully account for the fraction of immobilized receptors as determined by FRAP after LTP (see Figures 1G and 2F). That is, the amount of immobilized photobleached GluR1-SEP at a spine after LTP is the same regardless of the order in which spine photobleaching or spine LTP induction is delivered first. Therefore, we conclude that the majority of the receptors incorporated into the synapse during LTP originate from extrasynaptic regions of the spine surface.

Discussion

A number of studies have examined the constitutive and regulated movement of AMPARs onto synapses (reviewed in (Bredt and Nicoll, 2003; Collingridge et al., 2004; Malinow and Malenka, 2002; Newpher and Ehlers, 2008; Sheng and Kim, 2002; Shepherd and Huganir, 2007; Triller and Choquet, 2005). While there is general consensus that the number of AMPARs at synapses can be regulated in plasticity, the mechanisms controlling their synaptic incorporation remain poorly understood. In particular, the path by which receptors reach synapses during LTP has not been resolved. Some studies suggest that during LTP, there is lateral movement of receptors from nearby dendritic membrane surfaces into synapses (Borgdorff and Choquet, 2002; Chen et al., 2000; Yudowski et al., 2007). However, other studies suggest that exocytosis of membranous compartments containing receptors, either near the synapse (Oh et al., 2006; Park et al., 2006; Serulle et al., 2007; Wang et al., 2008; Yang et al., 2008) or at the synapse (Gerges et al., 2006), is an essential feature of LTP. Here we show that both lateral movement and exocytosis of receptors occur during LTP. However, they are separated in time and space, and likely have different functions: lateral movement of receptors from non-synaptic spine surface enhances the number of receptors at the synapse; exocytosis of receptors occurs onto the dendrite, but these receptors are not incorporated into synapses; they likely serve to replenish the local extrasynaptic pool of receptors used during subsequent plasticity.

Several studies have shown that agents targeted to block exocytosis can inhibit LTP. Our results suggest that prolonged blockade of exocytosis (Kopec et al., 2007; Park et al., 2006) may deplete the pool of surface GluR1 receptors available for synaptic incorporation, and thus block LTP. Acute introduction of agents that block exocytosis (Lledo et al., 1998; Park et al., 2004; Wang et al., 2008; Yang et al., 2008) may block surface appearance of molecules other than AMPARs and thereby block LTP, or these agents may perturb processes other than exocytosis that are necessary for LTP.

Our study finds that the majority of AMPARs incorporated into synapses during LTP contain GluR1, while AMPARs lacking GluR1 replace a fraction of synaptic receptors constitutively. A recent study questions the prevalence and role of AMPARs lacking GluR1 (Lu et al., 2009). However, their methods and logic do not measure directly the role or number of AMPARs lacking GluR1 at synapses. For instance, using their logic, acute

genomic loss of GluR2 should lead to no AMPAR-mediated synaptic transmission, which is not the case. We find that GluR1-containing AMPARs originating from the spine surface move into the synapse during LTP. This suggests that the magnitude of LTP may depend on the number of GluR1 on the extrasynaptic spine region (Yang et al., 2008). Factors that control this pool size could be the size of the spine or constitutive movement of GluR1 receptors onto the spine surface (Ehlers et al., 2007). The mobility of GluR1-SEP receptors from the dendrite to the extrasynaptic spine is fairly rapid. Thus, exocytosis of GluR1-containing receptors onto the dendrite, as we show occurs during LTP, will also control the spine GluR1 density during subsequent bouts of plasticity. Our results are consistent with a model in which LTP transiently creates synapse-specific "slots" that capture passively diffusing GluR1-containing AMPARs from the nearby spine membrane.

Experimental Procedures

Constructs

pCI-GluR1-SEP, pCI-GluR2-SEP and pCI-DsRed were cloned as described previously (Kopec et al., 2006). *Sindbis* virus dual promoter-driven expression of GluR1-SEP/GluR2-SEP and tdTomato was prepared as described previously (Kopec et al., 2007). Botulinum neurotoxin serotype A light chain (BoNT/A-LC, kindly provided by Dr. Mauricio Montal) was cloned into pCI (Promega).

Preparation

Organotypic hippocampal slice cultures were prepared from postnatal day 6–8 rats as described previously (Shi et al., 1999). After 13–20 days in culture, cells were either transfected by biolistic gene transfer (Gene gun; Bio-Rad) or electroporation (Plasmid DNA was directly injected into slice cultures with picospritzer (General Value Corporation) and electroporated into cells with 10 pulses (60 V, 50 μs) at 10 Hz (ECM; Harvard Apparatus).), or infected with *Sindbis* virus to express individual AMPAR subunits (GluR1 or GluR2) tagged on their amino-terminus with Super Ecliptic pHluorin (SEP), along with a cytoplasmic marker (DsRed or tdTomato) for 2–3 days (2 days for *Sindbis* virus).

Imaging

Either z-stack (Figures 1, 2, 3, S2, S3 and S4 in the Supplemental Data) or single plane (Figures 4, 5 and 6) images of hippocampal CA1 pyramidal neurons were acquired on a custom-built or commercial (Prairie) two-photon laser-scanning microscope using a Ti:Sapphire laser mode-locked to 910 nm (Chameleon; Coherent) in constant perfusion of artificial cerebrospinal fluid (ACSF: 119 mM NaCl, 26 mM $NaHCO_3$, 1 mM NaH_2PO_4, 11 mM D-glucose, 2.5 mM KCl, 4 mM $CaCl_2$, 4 mM $MgCl_2$ and 1.25 mM $NaHPO_4$ aerated with 95% O_2 and 5% CO_2) at 30° C. Either 40× or 60× objective lens (Olympus) was used to acquire images with 5× optical zoom. Both epi- and transfluorescence photons were collected by photomultiplier tubes and summed. The frequency of image capture is indicated in each figure, and ranges from every 2 sec to every 2 min.

Photobleaching of spines was achieved with repetitive xy scanning of a region of interest (ROI) at high illumination intensity (at 910 nm) for ~2 sec. Photobleaching of dendrites was achieved with repetitive xyz scanning of an ROI at high illumination intensity for ~3–5 min.

Chemical LTP

Chemical LTP (cLTP) was induced as described previously (Kopec et al., 2006; Kopec et al., 2007). Briefly, baseline images were acquired in basal ACSF with 4 μM 2-chloroadenosine (Sigma) at 10 min prior to cLTP induction. At time 0 min, the perfusion was switched to cLTP induction solution (ACSF with 0 mM Mg^{2+}, 4 mM Ca^{2+}, 50 μM

forskolin (Calbiochem or Sigma), 100 μM picrotoxin (Sigma) and 100 nM rolipram (Calbiochem)). At 16 min, the solution was switched back to basal ACSF.

LTP by two-photon glutamate uncaging

LTP by glutamate uncaging was induced as described previously (Harvey and Svoboda, 2007). Briefly, 2.5 mM 4-methoxy-7-nitroindolinyl (MNI)-caged-L-glutamate (Tocris) and 1 μM tetrodotoxin (TTX; Ascent Scientific or Tocris) were added to ACSF either with 0 mM added Mg^{2+} and 4 mM Ca^{2+} (Figure 2, 4 and 6) or with 1 mM Mg^{2+} and 2 mM Ca^{2+} (Figure 5). One ms-long 30 uncaging laser pulses (Ti:Sapphire mode-locked to 720 nm) were delivered at ~0.5 μm from the spine away from dendrites at the rate of 0.5 Hz. For the experiments in Figure 4, 5 and 6, single plane images were repetitively (~2 sec/frame) acquired with one laser (at 910 nm), while uncaging laser pulses were delivered independently with a second laser (at 720 nm). For the experiments in Figure 5, 1 ms-long 30 uncaging laser pulses were paired with postsynaptic depolarization to 0 mV. The intensity of uncaging laser was controlled with electro-optical modulators (Pockels cells; Conoptics).

NH_4Cl application

Baseline images were acquired in basal pH 7.4 ACSF with 4 μM 2-chloroadenosine. Dendritic regions (~40 μm) were either photobleached or left untouched, and pH 7.4 NH_4Cl (50 mM) containing 4 μM 2-chloroadenosine was bath applied to alkalinize intracellular acidic compartments.

Electrophysiology

Whole-cell recordings were made in basal ACSF (2 mM $CaCl_2$ and 1 mM $MgCl_2$) containing 2.5 mM MNI-caged-L-glutamate and 1 μM TTX at 30° C with an Axopatch- 1D amplifier (Axon Instruments). Patch recording pipettes (~3–6 MΩ) were filled with internal solution containing 115 mM cesium methanesulfonate, 20 mM CsCl, 10 mM HEPES, 2.5 mM $MgCl_2$, 4 mM Na_2ATP, 0.4 mM Na_3GTP, 10 mM sodium phosphocreatine and 0.6 mM EGTA (pH 7.2). Uncaging-evoked responses from a spine and dendrite were recorded at −60 mV to measure AMPAR-mediated responses. For spine responses, 1 ms-long laser pulse was given every 20 sec, while for dendritic responses, either 1 ms-long 3 uncaging laser pulses separated by 1 sec or a single laser pulse was given every 20 sec and results were pooled. The amplitudes were determined as the difference between the peak of an uncaging-evoked response and the mean current amplitude over 100-ms window before an uncaging stimulus.

Data analysis

Images were analyzed using custom written software in MatLab (MathWorks). Background-subtracted and leak-corrected red and green fluorescence was measured for spines and dendrites as previously described (Kopec et al., 2006; Kopec et al., 2007). For spine photobleaching experiments, integrated red and green fluorescence in photobleached spines was normalized to other non-photobleached spines at each time point to correct for possible fluorescence decay during repetitive image acquisition. Fluorescence recovery was measured as spine integrated green fluorescence normalized to spine integrated red fluorescence unless noted otherwise. For dendrite photobleaching experiments, integrated green fluorescence was normalized at each time point to non-photobleached dendrites to correct for possible fluorescence decay during repetitive image acquisition. Spine volume was measured as spine integrated red fluorescence normalized to integrated red fluorescence of primary dendrites. Each FRAP plot was fitted to dual-exponential curves according to the following equation with SigmaPlot (SPSS)

$$F(t)=F(0)+p(1-e^{-t/\tau f})+q(1-e^{-t/\tau s})$$

where F(0) is fluorescence intensity at time 0 min, p and q are relative size of fast and slow pools, and τf and τs are the recovery time constants for the fast and slow pools.

For LTP experiments, comparisons in spine volume and SEP-tagged AMPARs on spines were made between baseline (before) and 40 min after LTP induction (after).

Exocytotic events were identified as rapid appearance of SEP fluorescence that lasted more than 2 sec.

All data are presented as mean ± s.e.m. n indicates the number of spines analyzed unless noted otherwise. P values were obtained from Wilcoxon signed rank test for paired samples and Wilcoxon rank sum test for non-paired samples with MatLab (MathWorks) unless noted otherwise. Comparisons of FRAP were made at 30 min time points.

Supplementary Material

Refer to Web version on PubMed Central for supplementary material.

Acknowledgments

We thank Nancy Dawkins and Irina Hunton for technical support, Dr. Mauricio Montal for the BoNT/A-LC construct, Dr. Jeff Isaacson and past and current members of the Malinow laboratory for helpful discussions and critical review of the manuscript. This work was supported by an Elizabeth Sloan Livingston Fellowship (H.M.) and National Institute of Health (R.M.).

References

Adesnik H, Nicoll RA, England PM. Photoinactivation of native AMPA receptors reveals their real-time trafficking. Neuron 2005;48:977–985. [PubMed: 16364901]

Andersen P, Sundberg SH, Sveen O, Wigstrom H. Specific long-lasting potentiation of synaptic transmission in hippocampal slices. Nature 1977;266:736–737. [PubMed: 195210]

Andrasfalvy BK, Magee JC. Changes in AMPA receptor currents following LTP induction on rat CA1 pyramidal neurones. J Physiol 2004;559:543–554. [PubMed: 15235093]

Ashby MC, De La Rue SA, Ralph GS, Uney J, Collingridge GL, Henley JM. Removal of AMPA receptors (AMPARs) from synapses is preceded by transient endocytosis of extrasynaptic AMPARs. J Neurosci 2004;24:5172–5176. [PubMed: 15175386]

Ashby MC, Maier SR, Nishimune A, Henley JM. Lateral diffusion drives constitutive exchange of AMPA receptors at dendritic spines and is regulated by spine morphology. J Neurosci 2006;26:7046–7055. [PubMed: 16807334]

Borgdorff AJ, Choquet D. Regulation of AMPA receptor lateral movements. Nature 2002;417:649–653. [PubMed: 12050666]

Bredt DS, Nicoll RA. AMPA receptor trafficking at excitatory synapses. Neuron 2003;40:361–379. [PubMed: 14556714]

Chen L, Chetkovich DM, Petralia RS, Sweeney NT, Kawasaki Y, Wenthold RJ, Bredt DS, Nicoll RA. Stargazin regulates synaptic targeting of AMPA receptors by two distinct mechanisms. Nature 2000;408:936–943. [PubMed: 11140673]

Collingridge GL, Isaac JT, Wang YT. Receptor trafficking and synaptic plasticity. Nat Rev Neurosci 2004;5:952–962. [PubMed: 15550950]

Dean C, Liu H, Mark Dunning F, Chang PY, Jackson MB, Chapman ER. Synaptotagmin-IV modulates synaptic function and long-term potentiation by regulating BDNF release. Nat Neurosci. 2009

Ehlers MD, Heine M, Groc L, Lee MC, Choquet D. Diffusional trapping of GluR1 AMPA receptors by input-specific synaptic activity. Neuron 2007;54:447–460. [PubMed: 17481397]

Fernandez-Alfonso T, Ryan TA. A heterogeneous “resting” pool of synaptic vesicles that is dynamically interchanged across boutons in mammalian CNS synapses. Brain Cell Biol 2008;36:87–100. [PubMed: 18941900]

Gerges NZ, Backos DS, Rupasinghe CN, Spaller MR, Esteban JA. Dual role of the exocyst in AMPA receptor targeting and insertion into the postsynaptic membrane. Embo J 2006;25:1623–1634. [PubMed: 16601687]

Harvey CD, Svoboda K. Locally dynamic synaptic learning rules in pyramidal neuron dendrites. Nature 2007;450:1195–1200. [PubMed: 18097401]

Hayashi Y, Shi SH, Esteban JA, Piccini A, Poncer JC, Malinow R. Driving AMPA receptors into synapses by LTP and CaMKII: requirement for GluR1 and PDZ domain interaction. Science 2000;287:2262–2267. [PubMed: 10731148]

Heine M, Groc L, Frischknecht R, Beique JC, Lounis B, Rumbaugh G, Huganir RL, Cognet L, Choquet D. Surface mobility of postsynaptic AMPARs tunes synaptic transmission. Science 2008;320:201–205. [PubMed: 18403705]

Kopec CD, Li B, Wei W, Boehm J, Malinow R. Glutamate receptor exocytosis and spine enlargement during chemically induced long-term potentiation. J Neurosci 2006;26:2000–2009. [PubMed: 16481433]

Kopec CD, Real E, Kessels HW, Malinow R. GluR1 links structural and functional plasticity at excitatory synapses. J Neurosci 2007;27:13706–13718. [PubMed: 18077682]

Lledo PM, Zhang X, Sudhof TC, Malenka RC, Nicoll RA. Postsynaptic membrane fusion and long-term potentiation. Science 1998;279:399–403. [PubMed: 9430593]

Lu W, Shi Y, Jackson AC, Bjorgan K, During MJ, Sprengel R, Seeburg PH, Nicoll RA. Subunit composition of synaptic AMPA receptors revealed by a single-cell genetic approach. Neuron 2009;62:254–268. [PubMed: 19409270]

Malinow R, Malenka RC. AMPA receptor trafficking and synaptic plasticity. Annu Rev Neurosci 2002;25:103–126. [PubMed: 12052905]

Matsuzaki M, Honkura N, Ellis-Davies GC, Kasai H. Structural basis of long-term potentiation in single dendritic spines. Nature 2004;429:761–766. [PubMed: 15190253]

Newpher TM, Ehlers MD. Glutamate receptor dynamics in dendritic microdomains. Neuron 2008;58:472–497. [PubMed: 18498731]

Oh MC, Derkach VA, Guire ES, Soderling TR. Extrasynaptic membrane trafficking regulated by GluR1 serine 845 phosphorylation primes AMPA receptors for long-term potentiation. J Biol Chem 2006;281:752–758. [PubMed: 16272153]

Park M, Penick EC, Edwards JG, Kauer JA, Ehlers MD. Recycling endosomes supply AMPA receptors for LTP. Science 2004;305:1972–1975. [PubMed: 15448273]

Park M, Salgado JM, Ostroff L, Helton TD, Robinson CG, Harris KM, Ehlers MD. Plasticity-induced growth of dendritic spines by exocytic trafficking from recycling endosomes. Neuron 2006;52:817–830. [PubMed: 17145503]

Passafaro M, Piech V, Sheng M. Subunit-specific temporal and spatial patterns of AMPA receptor exocytosis in hippocampal neurons. Nat Neurosci 2001;4:917–926. [PubMed: 11528423]

Petralia RS, Wenthold RJ. Light and electron immunocytochemical localization of AMPA-selective glutamate receptors in the rat brain. J Comp Neurol 1992;318:329–354. [PubMed: 1374769]

Serulle Y, Zhang S, Ninan I, Puzzo D, McCarthy M, Khatri L, Arancio O, Ziff EB. A GluR1-cGKII interaction regulates AMPA receptor trafficking. Neuron 2007;56:670–688. [PubMed: 18031684]

Sharma K, Fong DK, Craig AM. Postsynaptic protein mobility in dendritic spines: long-term regulation by synaptic NMDA receptor activation. Mol Cell Neurosci 2006;31:702–712. [PubMed: 16504537]

Sheng M, Kim MJ. Postsynaptic signaling and plasticity mechanisms. Science 2002;298:776–780. [PubMed: 12399578]

Shepherd JD, Huganir RL. The cell biology of synaptic plasticity: AMPA receptor trafficking. Annu Rev Cell Dev Biol 2007;23:613–643. [PubMed: 17506699]

Shi S, Hayashi Y, Esteban JA, Malinow R. Subunit-specific rules governing AMPA receptor trafficking to synapses in hippocampal pyramidal neurons. Cell 2001;105:331–343. [PubMed: 11348590]

Triller A, Choquet D. Surface trafficking of receptors between synaptic and extrasynaptic membranes: and yet they do move! Trends Neurosci 2005;28:133–139. [PubMed: 15749166]

Wang Z, Edwards JG, Riley N, Provance DW Jr, Karcher R, Li XD, Davison IG, Ikebe M, Mercer JA, Kauer JA, Ehlers MD. Myosin Vb mobilizes recycling endosomes and AMPA receptors for postsynaptic plasticity. Cell 2008;135:535–548. [PubMed: 18984164]

Yang Y, Wang XB, Frerking M, Zhou Q. Delivery of AMPA receptors to perisynaptic sites precedes the full expression of long-term potentiation. Proc Natl Acad Sci U S A 2008;105:11388–11393. [PubMed: 18682558]

Yudowski GA, Puthenveedu MA, Leonoudakis D, Panicker S, Thorn KS, Beattie EC, von Zastrow M. Real-time imaging of discrete exocytic events mediating surface delivery of AMPA receptors. J Neurosci 2007;27:11112–11121. [PubMed: 17928453]

Zamanillo D, Sprengel R, Hvalby O, Jensen V, Burnashev N, Rozov A, Kaiser KM, Koster HJ, Borchardt T, Worley P, et al. Importance of AMPA receptors for hippocampal synaptic plasticity but not for spatial learning. Science 1999;284:1805–1811. [PubMed: 10364547]

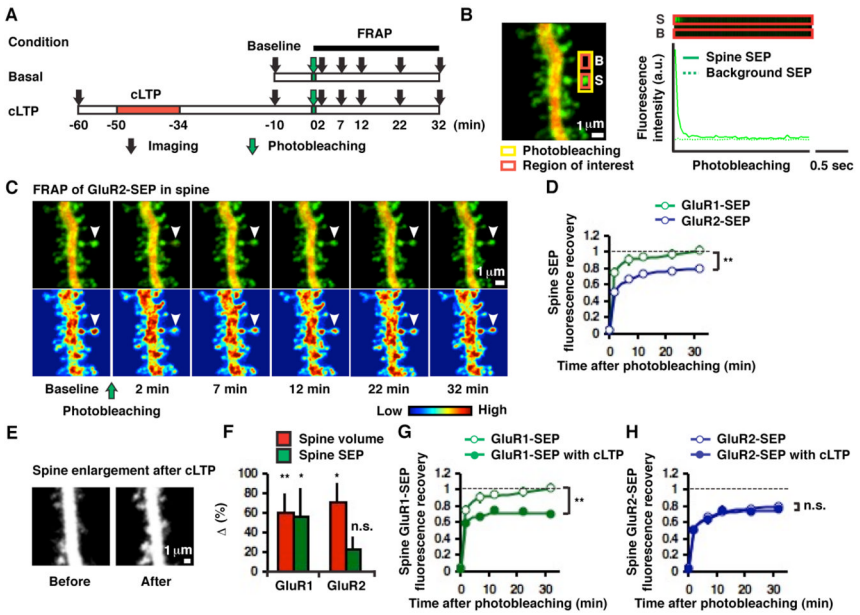

Figure 1. Subunit-specific AMPAR mobility on spines before and after cLTP

(A) Experimental design. (B) Example of a GluR2-SEP-expressing hippocampal CA1 pyramidal neuron and photobleaching of spine GluR2-SEP. S and B indicate spine and background, respectively. (C) Time-lapse images following photobleaching spine GluR2-SEP. Top and bottom panels show dual-color images and pseudo-color-coded SEP intensity images, respectively. Arrowhead indicates the spine that has undergone photobleaching. (D) Distinct fluorescence recovery on spines between GluR1-SEP (n = 14, 4 cells) and GluR2-SEP (n = 17, 4 cells, **p < 0.01). (E) Example of structural potentiation at 40 min after cLTP. (F) Mean changes in spine volume (n = 21, 8 cells for GluR1-SEP-expressing cell, **p < 0.01; n = 13, 3 cells for GluR2-SEP-expressing cell, *p < 0.05) and SEP-tagged AMPARs on spines (n = 21, 8 cells for GluR1-SEP, *p < 0.05; n = 13, 3 cells for GluR2-SEP, p = 0.19) following cLTP. (G) FRAP of GluR1-SEP obtained 50 min after LTP induction shows a significant synaptic immobile pool at the spine (n = 14, 4 cells for before cLTP; n = 21, 8 cells for after cLTP, **p < 0.01). (H) GluR2-SEP mobility on a spine is not affected by cLTP (n = 17, 4 cells for before cLTP; n = 14, 4 cells for after cLTP, p = 0.51).

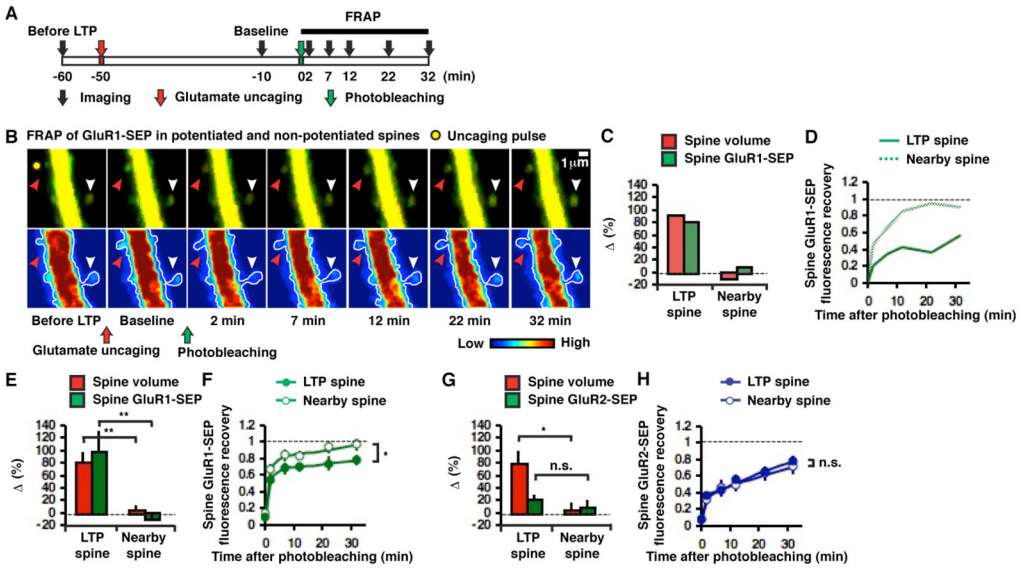

Figure 2. Input-specific reduction of GluR1-SEP mobility on spines after two-photon glutamate-uncaging-evoked LTP

(A) Experimental design. (B) Example of glutamate uncaging-evoked LTP (two-photon laser pulse location indicated by yellow filled circle) and FRAP in potentiated (red arrowhead) and nearby non-potentiated (white arrowhead) spines. Baseline image obtained 10 min before FRAP was captured 40 min after LTP induction. (C) Change in volume and GluR1-SEP in the potentiated and nearby non-potentiated spines shown in B (40 min after LTP induction). (D) Fluorescence recovery of GluR1-SEP after photobleaching the potentiated and non-potentiated spines shown in B. (E) Mean changes in spine volume and GluR1-SEP in potentiated (n = 14, 10 cells) and non-potentiated (n = 11, 7 cells, $^{**}p < 0.01$) spines (40 min after LTP induction). (F) Fluorescence recovery of GluR1-SEP after photobleaching in potentiated (n = 14, 10 cells) and non-potentiated (n = 11, 7 cells, $^{*}p < 0.05$) spines. (G) Mean changes in spine volume and GluR2-SEP in potentiated (n = 8, 3 cells) and non-potentiated (n = 8, 4 cells, $^{*}p < 0.05$, p = 0.44, respectively) spines (40 min after LTP induction). (H) Fluorescence recovery of GluR2-SEP after photobleaching in potentiated (n = 8, 3 cells) and non-potentiated (n = 8, 4 cells, p = 0.51) spines.

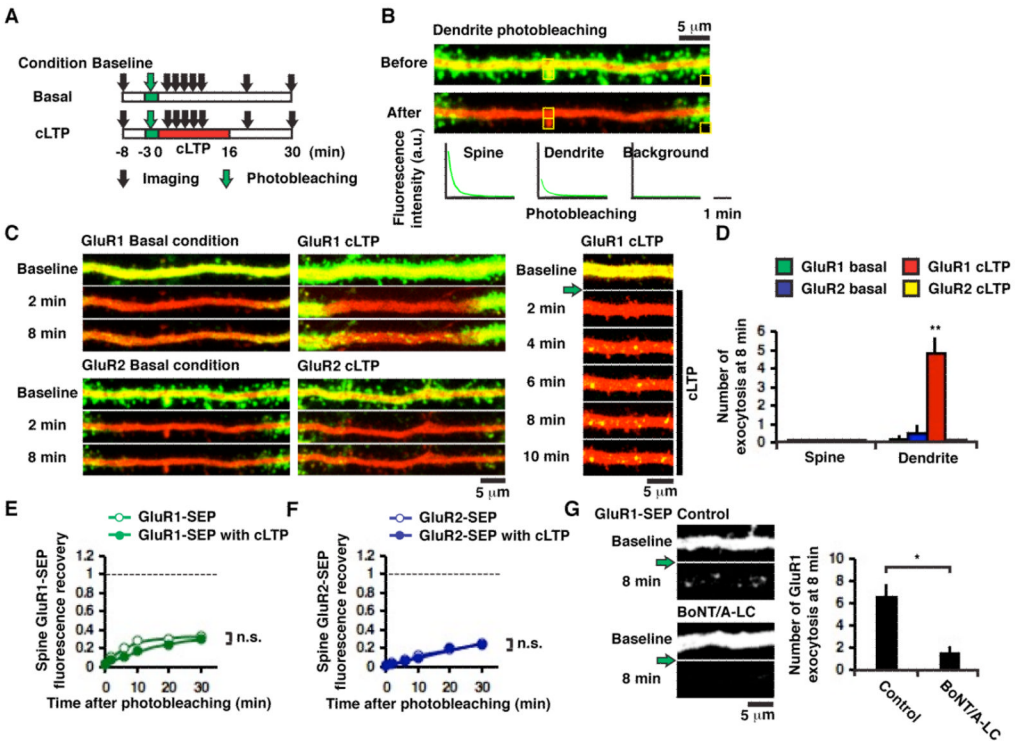

Figure 3. Subunit-specific AMPAR exocytosis onto dendrites during cLTP

(A) Experimental design. (B) Example of photobleaching dendrite GluR2-SEP in a hippocampal CA1 pyramidal neuron. (C) Examples of subunit-specific and activity-dependent AMPAR exocytosis; images captured every 2 min. Green arrow indicates dendrite photobleaching. (D) Number of exocytotic events within 12 μm from the center of photobleached region (~25 μm) at 8 min after cLTP induction (5 cells for GluR1-SEP basal condition, 4 cells for GluR2-SEP basal condition, 5 cells for GluR1-SEP cLTP and 3 cells for GluR2-SEP cLTP, **$p < 0.01$, Kruskal-Wallis test). (E) Fluorescence recovery of spine GluR1-SEP with (n = 33, 5 cells) and without cLTP (n = 24, 4 cells, $p = 0.56$). (F) Fluorescence recovery of spine GluR2-SEP with (n = 31, 3 cells) and without cLTP (n = 43, 4 cells, $p = 0.26$). Spine integrated green fluorescence was not normalized to spine integrated red fluorescence to avoid underestimation of spine AMPAR-SEP recovery in cLTP conditions. (G) Left: Example of GluR1-SEP exocytotic events without (control) or with coexpression of BoNT/A-LC. Images were acquired at 5 min prior to (baseline), and 8 min after photobleaching and cLTP induction (8 min). Green arrow indicates dendrite photobleaching. Right: Number of GluR1-SEP exocytotic events within 30 μm from the center of photobleached region (~40 μm) without (control, 5 cells) and with co-expression of BoNT/A-LC (7 cells, *$p < 0.05$).

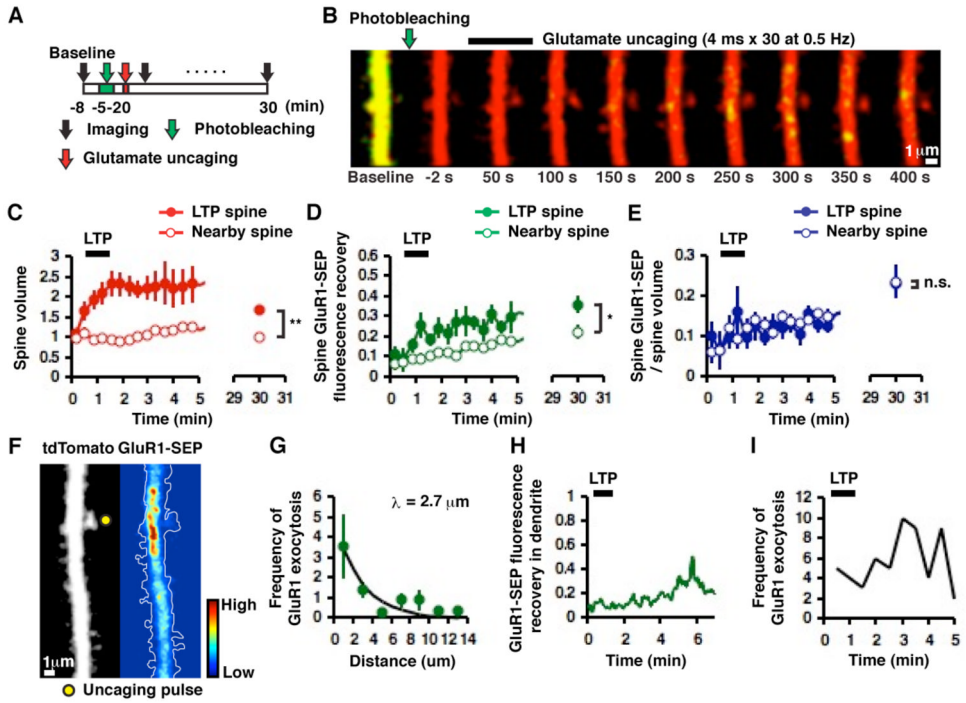

Figure 4. GluR1 exocytosis occurs primarily on dendrites during two-photon glutamate uncaging-evoked LTP and is compartmentalized to a stretch of dendrite

(A) Experimental design (images acquired at ~2 sec/frame). (B) Example of time-lapse images of highly compartmentalized GluR1 exocytosis along with an increase in spine volume mediated by single-spine LTP. Note that spine enlargement precedes GluR1 exocytosis. (C) Mean changes in spine volume in potentiated (n = 9, 8 cells) and nearby non-potentiated (n = 8, 5 cells, **p < 0.01) spines. (D) Fluorescence recovery of GluR1-SEP in potentiated (n = 9, 8 cells) and nearby non-potentiated (n = 8, 5 cells *p < 0.05) spines after photobleaching dendrites. (E) Mean changes in spine GluR1-SEP/volume in potentiated (n = 9, 8 cells) and non-potentiated (n = 8, 5 cells, p = 0.96) spines. (F) Example of compartmentalized GluR1 exocytosis. Left panel shows the morphology of a hippocampal CA1 pyramidal neuron and right panel shows a pseudo-color-coded rate/ intensity map of GluR1 exocytosis (two-photon laser pulse location indicated by yellow filled circle). These images were obtained by integrating over 200 time-lapse images acquired over ~7 min. (G) Frequency of GluR1 exocytosis within 5 min of glutamate uncaging plotted as a function of distance from a potentiated spine (binned by 2 μm, 8 cells). Exponential fit with a length constant λ = 2.70 μm. (H) Time-course of GluR1-SEP fluorescence recovery in dendrites next to the potentiated spine in B. Note the transient increase in the GluR1-SEP signal minutes following glutamate uncaging. (I) Frequency of GluR1 exocytosis after glutamate uncaging plotted as a function of time. The number of events was summed across 8 cells. Note the frequency of GluR1 exocytosis increases considerably after the last laser pulse of glutamate uncaging.

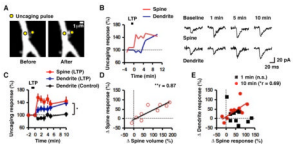

Figure 5. Exocytosis of endogenous AMPARs detected by two-photon glutamate uncaging-evoked responses on dendrites

(A) Example of structural changes following glutamate uncaging-evoked LTP; glutamate uncaging-mediated responses obtained before and after LTP at locations indicated by the yellow filled circles. (B) Example of AMPAR-mediated currents in the spine and dendrite before and after glutamate uncaging-evoked LTP. Right panel shows response traces (average of 3 responses). (C) Mean changes in AMPAR-mediated inward currents in spines (n = 10, 10 cells) and dendrites (n = 17, 17 cells) following glutamate uncaging-evoked LTP. Black points indicate dendrite responses obtained in the absence of the LTP induction protocol (n = 7, 7 cells, *p < 0.05). Each point is an average of 3 responses obtained every 20 sec. (D) Correlation between changes in spine volume and spine responses (n = 9, 9 cells, r = 0.87, **p < 0.01). (E) Significant correlation between changes in spine responses and changes in dendrite responses at 10 min (n = 10, 10 cells, r = 0.69, *p < 0.05) but not at 1 min after LTP induction (n = 10, 10 cells, p = 0.16).

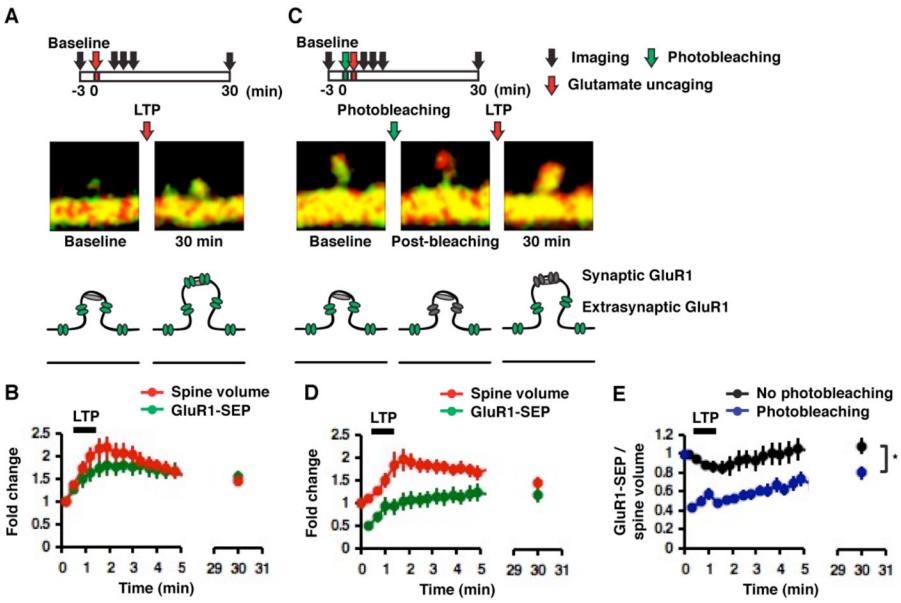

Figure 6. The majority of synaptic AMPARs originate from a spine surface GluR1-containing receptor pool

(A) Example of an increase in spine volume and GluR1-SEP following two-photon glutamate uncaging-evoked LTP (images acquired at ~2 sec/frame). (B) Mean changes in spine volume and GluR1-SEP following glutamate uncaging-evoked LTP (n = 14, 12 cells). (C) Example of increases in spine volume and GluR1-SEP following photobleaching spines and glutamate uncaging-evoked LTP (images acquired at ~2 sec/frame). (D) Mean changes in spine volume and GluR1-SEP following photobleaching spines and glutamate uncaging-evoked LTP (n = 11, 9 cells). (E) Mean changes in spine GluR1-SEP/volume for glutamate uncaging-evoked LTP only (n = 14, 12 cells) and photobleaching plus glutamate uncaging-evoked LTP (n = 11, 9 cells, *$p < 0.05$).